Modification of energy transfer from Si nanocrystals to Er3+ near a Au thin film

Nakamura, Toshihiro
Imakita, Kenji
Fujii, Minoru
Hayashi, Shinji

(Citation)
Physical Review B,72(23):235412-235412

(Issue Date)
2005-12-08

(Resource Type)
journal article

(Version)
Version of Record

(URL)
https://hdl.handle.net/20.500.14094/90000090

Modification of energy transfer from Si nanocrystals to Er^{3+} near a Au thin film

Toshihiro Nakamura, Minoru Fujii,* Kenji Imakita, and Shinji Hayashi
Department of Electrical and Electronics Engineering, Faculty of Engineering, Kobe University, Rokkodai, Nada, Kobe 657-8501, Japan
(Received 22 June 2005; revised manuscript received 5 October 2005; published 8 December 2005)

The effects of a Au thin layer on the rate of energy transfer from Si nanocrystals (Si-nc's) to Er^{3+} were studied. The energy transfer rate was found to oscillate with increasing the separation between the active layer and the Au thin film. The period of the oscillation agreed well with that of the calculated radiative decay rates of Si-nc's at the energy transfer wavelength. The present results provide evidence that the rate of energy transfer from Si-nc's to Er^{3+} is proportional to the photonic mode density at the energy transfer wavelength and can be controlled by controlling the photonic environment.

DOI: 10.1103/PhysRevB.72.235412 PACS number(s): 78.67.Bf, 34.30.+h, 78.55.−m

I. INTRODUCTION

Sensitized excitation of Er^{3+} by the energy transfer from Si nanocrystals (Si-nc's) has been attracting a lot of attention[1–8] because it overcomes the small excitation cross section of Er^{3+}. One of the most promising applications of this phenomenon is a compact planer optical amplifier operating at the 1.54 μm range[9,10]; the size of an Er doped fiber amplifier used for long-distance optical telecommunication is greatly reduced because of the large absorption cross section of Si-nc's and the efficient energy transfer to Er^{3+}. The efficient energy transfer from Si-nc's to Er^{3+} and the inefficient energy transfer for the reverse direction are considered to arise from the modified electronic structures of the Si-nc's by the quantum size effects.

Intensive research has been done to understand the mechanism of sensitized excitation of Er^{3+} and the conditions needed to realize optical amplification. Pacifici *et al.*[11] constructed a model, which takes into account all possible transitions in and between Si-nc's and Er^{3+}, and clarified the conditions needed to realize optical amplification. In a previous work,[8] we studied the time transient of 1.54 μm photoluminescence (PL) of Er^{3+} after the excitation of Si-nc's and found that the intensity rises after finishing excitation, which evidences energy transfer from Si-nc's. Detailed analysis of the time transient of the PL revealed that there are two different energy transfer processes, i.e., fast and slow ones. The energy transfer rate of the fast process is larger than our time resolution (100 ns) and the mechanism is considered to be essentially the same as that in Er doped bulk Si crystals, i.e., an exciton is trapped to an Er^{3+} related center in the band gap of Si and transfers its energy by an Auger-like process. Since the process is mediated by trap centers, the energy transfer rate does not strongly depend on the size of the Si-nc's and inhomogeneously broadened PL bands of Si-nc's are quenched totally. The rate of the fast process is much larger than the radiative recombination rate of excitons in Si-nc's, resulting in complete quenching of the PL from Si-nc's.

In addition to the bulklike fast process, a slow energy transfer process, which is a characteristic process in the Si-nc's-Er system, exists. The energy transfer rate of this process can be measured from the rising part of the delayed luminescence from Er^{3+}, and is in the range of several tenths to several hundredths of microseconds. It was found that the energy transfer rate of the process is proportional to the recombination rate of excitons in Si-nc's.[12] The proportionality strongly suggests that the process is a Förster type Coulombic interaction[13] between excitons and Er^{3+}. In contrast to the fast process, the slow process is a direct interaction between excitons and Er^{3+}. The direct interaction results in a strong size dependence of the energy transfer rate. Since the electronic states of Er^{3+} are discrete and the band gap energies of Si-nc's are distributed by size distribution, there should be optimum sizes of Si-nc's which can transfer energy resonantly to Er^{3+} within the size distribution. This resonant energy transfer appears as spectral holes in inhomegeneously broadened PL bands of Si-nc's at low temperatures.[14] The energy transfer rate of the slow process is comparable to the decay rates of excitons in Si-nc's. Therefore, the luminescence from Si-nc's is not completely quenched by the energy transfer. The effect of the energy transfer appears as a shortening of the lifetime of exciton luminescence, and from the degree of the shortening, the energy transfer rate can be estimated.

Recently, it has been proposed that Förster energy transfer can be modified by microcavities and metal structures in which the local photonic environment is altered.[15–18] Hopmeier *et al.*[19] showed that the energy transfer between organic molecules is enhanced if they are located in a dielectric microcavity. Furthermore, Andrew and Barnes[20] demonstrated that the energy transfer rate depends linearly on the radiative rate of an energy donor in a metal microcavity. On the other hand, Dood *et al.*[21] showed contradicting results, i.e., the energy transfer rate between Er^{3+} is not modified by its photonic environment when placed in a dielectric microcavity.

These studies have mainly been made on molecules and ions. It is of interest whether or not the same scenario works on other systems such as excitons in semiconductor nanocrystals. As mentioned above, the slow energy transfer from Si-nc's to Er^{3+} is considered to be due to the Förster type process, and thus is a good system for the study of the effect of the photonic environment on the energy transfer rate.

The main purpose of this work is to investigate the effects of Au thin layers on the energy transfer rate from Si-nc's to Er^{3+}. We first study the effects on the decay rates of Si-nc's for the samples not containing Er. We will show that the

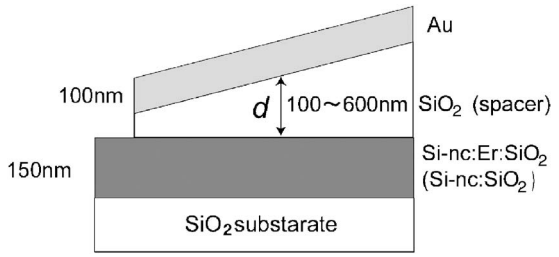

FIG. 1. Schematic representation of the sample structure. SiO_2 active layer containing Si-nc's and Er (Si-nc:Er:SiO_2) or Si-nc's (Si-nc:SiO_2) is deposited on a SiO_2 substrate. On the active layer, a SiO_2 spacer layer and a Au thin layer (100 nm) is deposited.

decay rates are strongly modified by placing a Au thin layer on top of the samples, and that the dependence of the rates on the distance between the samples and the Au layer is well explained by a theoretical model. We then study the effects of the Au layer on the energy transfer rate. We estimate the rate by two approaches, i.e., from PL time transients of energy donors (Si-nc's) and acceptors (Er^{3+}). We will demonstrate that the energy transfer rate oscillates depending on the sample-Au layer distance. We will show that the oscillation behavior of the energy transfer rate is in good agreement with that of the calculated radiative decay rate at 1.26 eV, where the energy transfer from Si-nc's to Er^{3+} is made.

II. EXPERIMENTAL PROCEDURE

Figure 1 shows a schematic illustration of the sample structure. An active layer consisting of SiO_2 films containing Si-nc's (Si-nc:SiO_2) or Si-nc's and Er (Si-nc:Er:SiO_2) were deposited on a SiO_2 substrate by the cosputtering of Si, SiO_2, and Er_2O_3.[3,4] The thickness of the films was about 150 nm. The films were then annealed in a nitrogen gas atmosphere for 30 min at 1200 °C to grow Si-nc's. In this method, the size of Si-nc's can be controlled by changing the excess Si concentration or the annealing temperature. In this work, the size was controlled so that the luminescence maximum of Si-nc's coincided with the excitation energy of the $^4I_{11/2}$ state of Er^{3+} (1.26 eV). The average size of Si-nc's (d_{Si}) was about 4.1 nm. Er concentration was fixed to 0.11 at. %. After the growth of Si-nc's by annealing, a SiO_2 spacer layer was deposited on the active layer by the sputtering method. The thickness of the layer (d) was changed from 100 to 600 nm continuously on a sample by controlling a shutter during the sputtering. Finally, a Au thin film (about 100 nm in thickness) was deposited by vacuum evaporation.

The PL spectra were measured using a single monochromator equipped with an InGaAs near-infrared diode array. The excitation source for all measurements was a 510 nm light from an optical parametric oscillator (OPO) pumped by the third harmonic of a neodium:yttrium-aluminum-garnet (Nd:YAG) laser (pulse energy 0.5 mJ/cm^2, pulse width 5 ns, and repetition frequency 20 Hz). In this wavelength, Er^{3+} is not directly excited by incident photons; only Er^{3+} having interaction with Si-nc's can be excited by the energy transfer from Si-nc's, while those not interacting with Si-nc's are not excited. For all the spectra, the spectral response of the detection system was corrected by the reference spectrum of a standard tungsten lamp. For the time response measurements, the luminescence signal was detected by a near-infrared photomultiplier (R5509-72, Hamamatsu) and the decay curve was recorded by a multichannel scalar (SR430 Stanford Research). The overall time resolution of the system was better than 100 ns. All measurements were performed at room temperature.

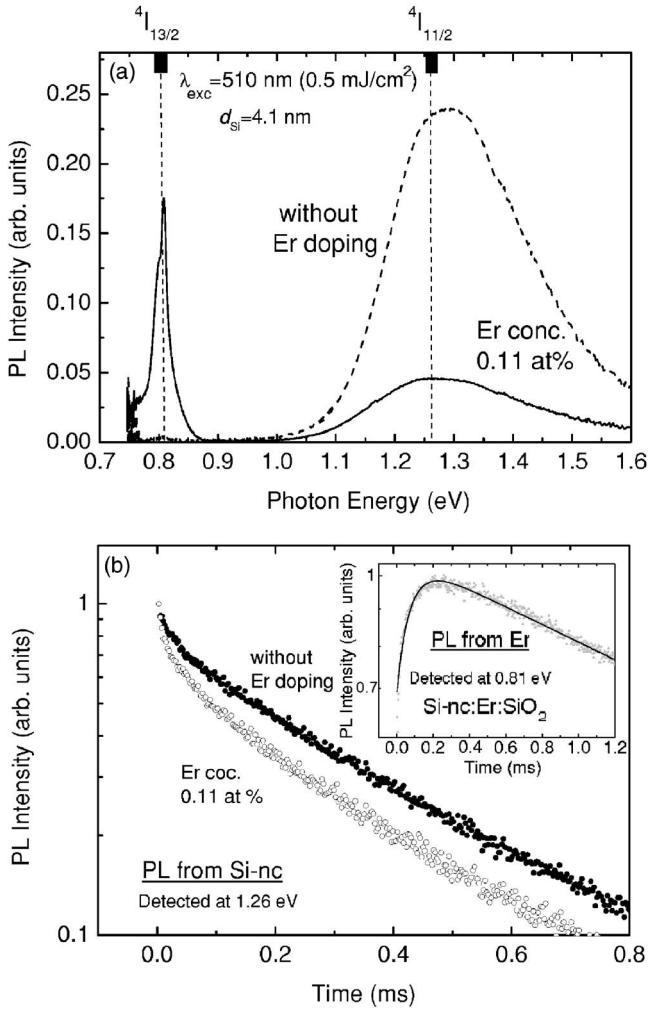

FIG. 2. (a) The PL spectra of a SiO_2 film containing Si-nc's (d_{Si}=4.1 nm) and that containing Si-nc's and Er (0.11 at. %). The broad emission band at around 1.27 eV is due to recombination of excitons in Si-nc's, and a sharp peak at 0.81 eV arises from intra 4-f shell transition of Er^{3+} ($^4I_{13/2} \rightarrow {}^4I_{15/2}$). (b) PL decay curves of Si-nc's at 1.26 eV for the sample containing and not containing Er. Inset shows a typical PL time transient of Er at 0.81 eV.

III. RESULTS AND DISCUSSION

A. Energy transfer from Si nanocrystals to Er^{3+}

Before starting the discussion on the effects of a Au layer, we will demonstrate the evidence of energy transfer from Si-nc's to Er^{3+} and show how to determine the energy transfer rate.[12] Figure 2(a) shows PL spectra of Si-nc:SiO_2 and Si-nc:Er:SiO_2 films. The broad emission band at around

1.27 eV is due to the recombination of excitons in Si-nc's and the sharp one at 0.81 eV is due to the intra-4*f* shell transition of Er^{3+}. We can see that the PL from Si-nc's is quenched by Er doping. The quenching is accompanied by a shortening of the lifetime, as can be seen in the PL decay curves in Fig. 2(b). The quenching and the shortening of the lifetime of the PL from Si-nc's by Er doping is strong evidence of the nonradiative energy transfer from Si-nc's to Er. If we assume that the shortening of the lifetime is due to the energy transfer to Er^{3+}, the energy transfer rate can be estimated from a change of the decay rates. Additional and more direct evidence of the energy transfer is obtained from the time transient of PL from Er^{3+} after the pulsed excitation of Si-nc's. The inset of Fig. 2(b) shows a typical time transient curve of PL from Er^{3+} at 0.81 eV. We can clearly see that PL intensity rises slowly after finishing the excitation. This PL delay is direct evidence that Er^{3+} is excited indirectly by the energy transfer from Si-nc's, and the energy transfer rate can be estimated from the rise time.

The time transients of PL from Er can be reproduced by a model which takes into account the two different energy transfer processes, i.e., fast and slow ones.[12] In the model, the time transient is expressed as

$$I(t) \propto \left(\frac{N_{Er}^{f}}{N_{\mathrm{Er}}^{s}} + \frac{W_{\mathrm{tr}}^{s}}{W_{\mathrm{tr}}^{s} + W_{\mathrm{Si}} - W_{\mathrm{Er}}}\right)\exp(-W_{\mathrm{Er}}t) - \frac{W_{\mathrm{tr}}^{s}}{W_{\mathrm{tr}}^{s} + W_{\mathrm{Si}} - W_{\mathrm{Er}}}\exp[-(W_{\mathrm{tr}}^{s} + W_{\mathrm{Si}})t], \qquad (1)$$

where N_{Er}^{f} and N_{Er}^{s} denote the number of Er^{3+} contributing to the fast and slow processes, respectively, W_{tr}^{s} is the energy transfer rate of the slow process, W_{Si} is the recombination rate of Si-nc's when Er does not exist nearby, and W_{Er} is the relaxation rate of excited Er. The fast process is faster than our time resolution and thus the rate does not appear in the model. Among these parameters, W_{Si} is estimated from the decay curves of Si-nc:SiO_2 samples, while others can be estimated from the fitting. The solid curve in the inset of Fig. 2(b) is the result of the fitting. We see that the model can reproduce the experimental results quite well.

B. Effects of Au thin films on PL properties of Si nanocrystals

In this section, we will discuss the effects of a Au layer on the PL properties of Si-nc's in Si-nc:SiO_2 samples. The inset of Fig. 3(a) shows the PL decay curves at 1.26 eV for Si-nc:SiO_2 samples with a Au thin film. The spacer thicknesses are 120, 270, and 330 nm. We can see that the lifetime, as well as the shape of decay curves, depends strongly on the spacer thickness. In order to estimate the decay rate, the PL decay curves are fitted with the stretched exponential function,[22] which has been commonly used to estimate PL lifetime of Si-nc's. In Fig. 3(a), the decay rates estimated by the fitting are plotted as a function of the spacer thickness (closed squares). We see that the decay rates oscillate with increasing spacer thickness. For a comparison, the decay rate of the sample without the Au layer is shown by the horizontal dashed line.

In order to explain the origin of the variation of the PL decay rates, we calculated the decay rates from a model de-

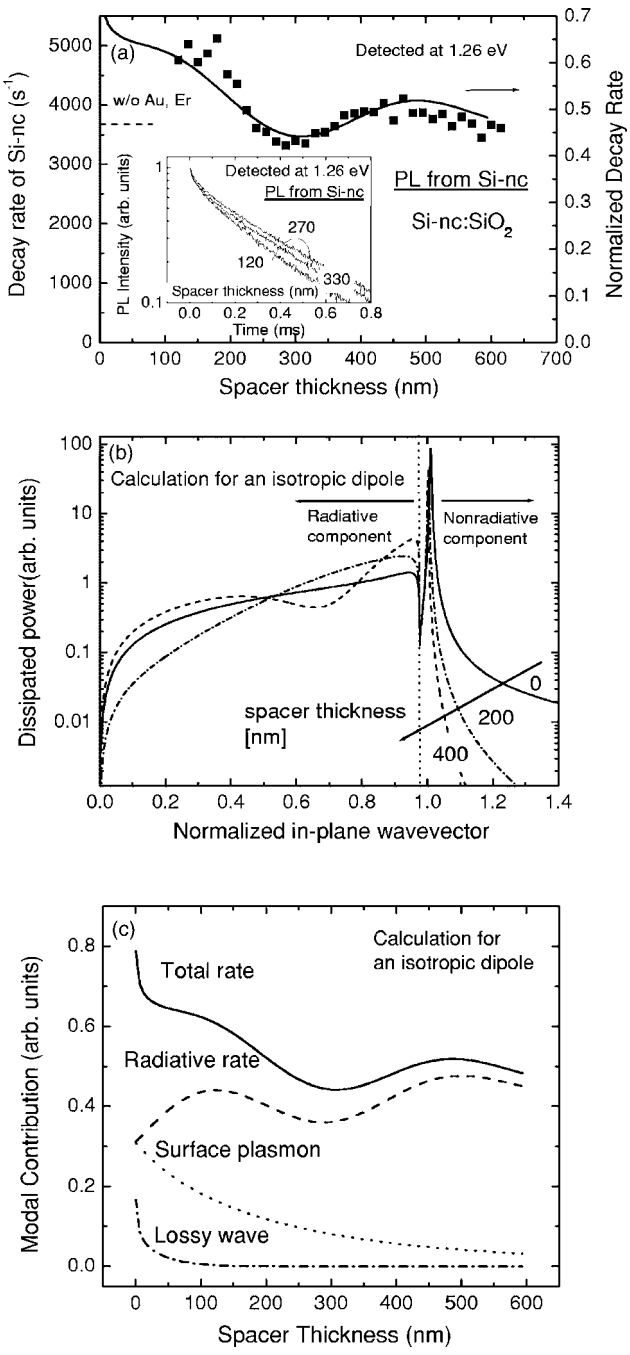

FIG. 3. (a) The PL decay rates of Si-nc's as a function of spacer thickness (closed squares). The decay rate without the Au thin film is shown by a horizontal dashed line (left axis). The solid curve represents the normalized decay rate calculated for an isotropic dipole emitting at 1.26 eV (right axis). In the inset, the PL decay curves of Si-nc's for various spacer thickness are shown. (b) A dissipated power spectrum at 1.26 eV for an isotropic dipole positioned at the center of an active layer as a function of normalized in-plane wave vector. (c) Spacer thickness dependence of the total decay rate (solid line), the radiative rate (dashed line), the rates of energy transfer to surface plasmon modes (dotted line), and lossy wave modes (dashed dotted line). In obtaining these rates, the contribution of dipoles positioned between the active layer/substrate and the active layer/spacer interfaces were averaged.

veloped by Chance *et al.*[23] In the calculation, emitters are treated as a point dipole positioned at a distance from the metal or dielectric surface in an arbitrary medium. The dipole field interferes with the field reflected by the surface, and the interference modifies the radiative rate of the dipole. In addition, when the dipole field couples to the surface plasmon modes in metal or guided wave modes, nonradiative energy transfer from the dipole to the modes occurs, which results of the increase of the decay rate. The power dissipation, i.e., the decay rate, of the dipole is obtained from the imaginary part of the electric field.[24] The dissipated power as a function of the in-plane wave vector is a measure of the power lost to each mode; the modes of the in-plane wave vectors smaller than the far field wave vector[25] are radiative, while those that are higher than that are nonradiative. The total decay rate is obtained by adding the power dissipated to all the modes or integrating over the whole wave vector range.

For practical calculation, we considered a four layer system shown in Fig. 1. The dielectric constants Au, the spacer, and the active layers used for the calculation are $\epsilon_{Au}=-46.2+3.62i$, $\epsilon_{SiO_2}=1.44$, and $\epsilon_{SiO_x}=1.48$, respectively.[26] The dielectric constant of the active layer was estimated by the Bruggeman effective medium theory.[27] Figure 3(b) shows the dissipated power spectra of an isotropic dipole emitting at 1.26 eV, positioned at the center of the active layer as a function of normalized in-plane wave vector (u), which is defined by an in-plane wave vector divided by a far-field wave vector. The spacer thickness is changed from 0 to 600 nm. In this system, the normalized in-plane wave vector from 0 to 0.97, which is the condition for total internal reflection at the active layer-substrate interface, corresponds to the propagating far-field components (radiative), while those larger than 0.97 correspond to the nonradiative components. The oscillation observed at $u<0.97$ for the spacer thickness of 400 nm is caused by the destructive or constructive interference of the dipole field with the reflected one. A sharp peak at around $u=1.1$ is due to the excitation of the surface plasmon mode at the Au-active layer interface, its intensity increases with the decrease of the spacer thickness because the fields accompanied by the surface plasmon mode decay exponentially from the interface.[25] The component of $u>1.1$ is the excitation of the lossy wave mode, which is the energy transfer to the electronic charge density oscillations.[25] The dissipation of power into the lossy wave modes rapidly increases as the spacer thickness decreases.[25]

In order to retain the information about the modal contribution of each mode to a total decay rate, we integrated the dissipated power over limited wave vector ranges. In obtaining these rates, the contributions of dipoles positioned in the 150 nm thick active layers were averaged. The contributions of the radiative mode, the excitation of the surface plasmon, and the lossy wave modes are shown in Fig. 3(c), together with the total dissipated power. We see that the radiative rate oscillates due to the interference between dipole fields and those reflected from the Au thin film. On the other hand, the excitation rates of the surface plasmon and lossy wave modes decrease monotonically with increasing spacer thickness.

In Fig. 3(a), the calculated total dissipated power (solid curve) is compared with experimentally obtained decay rates. We can see that they show very similar spacer thickness dependence, indicating that the observed large decay rates at the small spacer thickness are due to the coupling of excitons with the surface plasmon and lossy wave modes, and the oscillation of the rate at large spacer thickness is due to the oscillation of the radiative rate.

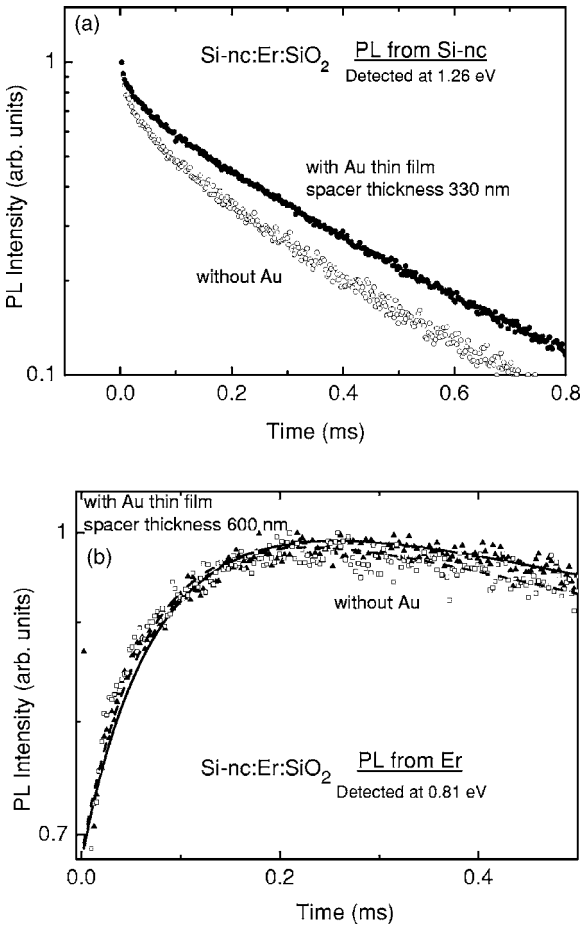

FIG. 4. (a) The PL decay curves of Si-nc's (1.26 eV) with (closed circles) and without (open circles) Au thin films for the samples containing Si-nc's and Er. The spacer thickness is 330 nm. (b) The PL time transients of Er^{3+} (0.81 eV) with (closed triangles) and without (open squares) Au thin films obtained for the same samples. The spacer thickness is 600 nm. The solid and dashed curves are the results of fitting (see Ref. 12).

C. Effects of Au thin films on energy transfer from Si nanocrystals to Er^{3+}

We are now ready to discuss the effects of a Au layer on the energy transfer from Si-nc's to Er^{3+}. Figures 4(a) and 4(b) show the time transients of PL from Si-nc's and Er^{3+}, respectively, for Si-nc:Er:SiO_2 samples covered or not covered by Au thin films. The spacer thickness is 330 and 600 nm, respectively. The lifetime of PL from Si-nc's becomes longer by the presence of the Au layer [Fig. 4(a)]. The effect of the Au layer also appears on the PL time transient of Er^{3+} [Fig. 4(b)]. Although not very clear, both the PL delay and decay time become longer by the Au layer.

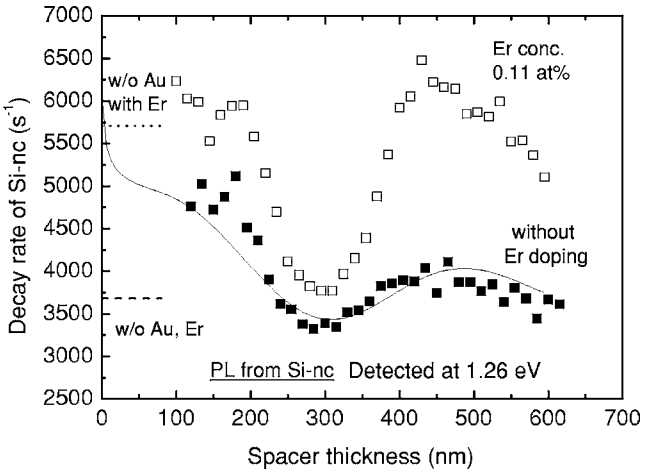

FIG. 5. The PL decay rates of a SiO_2 film containing Si-nc's (closed squares) and that containing Si-nc's and Er (open squares) at 1.26 eV as a function of spacer thickness. The decay rates of Si-nc:SiO_2 and Si-nc:Er:SiO_2 without Au thin films are shown by the horizontal dashed line and horizontal dotted line, respectively.

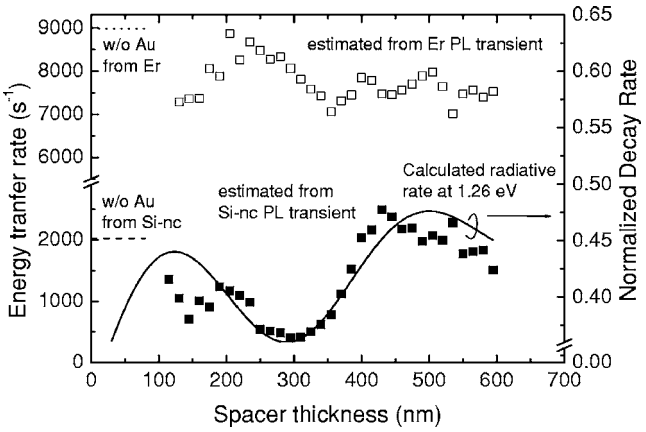

FIG. 6. Energy transfer rates estimated from the time transient of Er PL (open squares) and that estimated from decay rates of Si-nc's (closed squares) as a function of spacer thickness. The solid curve represents calculated radiative rate at 1.26 eV (right axis). Energy transfer rates estimated from Er PL and Si-nc's PL for the sample without Au thin films are shown by the horizontal dotted and horizontal dashed lines, respectively.

We first try to estimate the energy transfer rate from the decay rates of PL from Si-nc's. Figure 5 shows the decay rates of Si-nc's as a function of the spacer thickness for Si-nc:Er:SiO_2 samples (open squares). The decay rates are obtained by fitting the PL decay curves with a stretched exponential function. For comparison purposes, the decay rates of Si-nc's PL in Si-nc:SiO_2 samples are also shown (closed squares). We can clearly see that the decay rates of Si-nc:Er:SiO_2 samples oscillate with larger amplitudes than the samples not containing Er. The strong enhancement of the oscillation amplitude suggests that the energy transfer rate is strongly modified by the presence of the Au layer.

In the simplified model, the decay rates of Si-nc's PL for Si-nc:Er:SiO_2 samples are expressed as $W_{Si}+W_{ET}$, where W_{Si} and W_{ET} denote the decay rates in the absence of Er and the energy transfer rate, respectively. Therefore, by subtracting the decay rates of Si-nc's without Er from that with Er, W_{ET} can be estimated. Figure 6 shows the estimated energy transfer rate as a function of the spacer thickness (closed squares). We can see the oscillation of the energy transfer rate.

In order to understand the mechanism of the oscillation of the energy transfer rate, we compare the results with theoretical calculations. By comparing the results in Fig. 6 with the calculated decay rates at 1.26 eV shown in Fig. 3(c), we notice that the oscillation behavior of the energy transfer rate is very similar to that of the radiative decay rates of Si-nc's at 1.26 eV. The solid curve in Fig. 6 is the calculated radiative decay rate at 1.26 eV. The oscillation period of the calculated radiative rate is in good agreement with that of the energy transfer rates estimated from the time transient of Si-nc's PL. The similar oscillation behavior of the experimentally obtained energy transfer rate and the calculated radiative decay rate strongly suggests that a common mechanism stands behind them.

As discussed above, the oscillation of the radiative decay rate is due to the interference of the dipole fields and the reflected fields. Another explanation of this phenomenon is that the local photonic mode density (PMD) is modified due to the existence of a metal layer.[25,28–30] Since the radiative decay rate is proportional to the PMD, oscillation of the PMD results in the radiative decay rate. It is well known that the rate of a Förster type energy transfer is proportional to the radiative rate of the energy donor.[13] Therefore, if the radiative decay rate of a donor is modified by changing the PMD, the energy transfer rate is also modified with the same period. In the present system, the energy transfer from Si-nc's to Er^{3+} by the slow Förster type process is made mainly to the second excited state of Er^{3+} at 1.26 eV. Therefore, Si-nc's with the band gap energy of 1.26 eV are energy donors, and the energy transfer rate should be proportional to the PMD at 1.26 eV. We believe that the results shown in Fig. 6 prove the proportionality relation between the PMD and the energy transfer rate.

The results of Fig. 6 strongly suggest that control of the PMD is a possible approach to control the energy transfer rate. However, in the present samples, the energy transfer rate decreased in the wide spacer thickness range. An enhancement of the rate is expected to be possible by using a rough metal surface instead of a flat one. In our preliminary work on similar samples with rough metal films, the enhancement of the rate is obtained. Those results will be shown elsewhere.

In the present work, the energy transfer rate can also be estimated from the rising part of the PL time transients of Er^{3+}. To estimate the rate we fitted the curves by Eq. (1). For the fitting, W_{Si} obtained from decay curves of Si-nc's PL at 1.26 eV of Si-nc:SiO_2 samples with the same spacer thicknesses were used. The solid curves in Fig. 4(b) are the results of the fitting and reproduce the experimental results quite well. Open squares in Fig. 6 show the estimated energy transfer rates as a function of the spacer thickness. We see again the oscillation of the energy transfer rate. However, the absolute values of the rate are different from those estimated from Si-nc's PL. The decay curves of PL from Si-nc's are

determined by an ensemble of those having interaction with Er^{3+} and those not having interaction. The presence of Si-nc's without interaction with Er^{3+} suppresses the shortening of the measured lifetime, resulting in a seemingly smaller energy transfer rate.

In Fig. 6, the oscillation period of the rate estimated by the two methods do not agree perfectly. In the present samples, in addition to the energy transfer to the second excited $^4I_{11/2}$ state of Er^{3+} (1.26 eV), that to the third excited $^4I_{9/2}$ state (1.55 eV) is partially possible because of the broad PL bands of Si-nc's [see Fig. 2(a)]. The energy transfer rate estimated from the time transient of Er^{3+} PL thus reflects not only the rate to the $^4I_{11/2}$ state but also that to the $^4I_{9/2}$ state. The two energy transfer processes exhibit different spacer thickness dependence of the energy transfer rate, i.e., the oscillation period at 1.55 eV is smaller than that at 1.26 eV. We believe that the contribution of the third excited state to the energy transfer process modifies the oscillation behavior, and results in different spacer thickness dependence of the rate from that estimated from the decay curves of Si-nc's PL.

IV. CONCLUSION

The effects of a Au layer on the rate of Förster energy transfer from Si-nc's to Er^{3+} were studied. We found clear oscillation of the rate with the increasing thickness of the spacer layer between the active layer and the Au layer. The oscillation behavior of the radiative decay rate at the energy transfer wavelength agreed well with that of the energy transfer rate. Since the radiative rate is proportional to the photonic mode density, the present results provide the evidence that the energy transfer rate is proportional to the photonic mode density at the energy transfer wavelength. The present results suggest that the control of photonic environment is a promising approach to controlling the energy transfer rate from Si-nc's to Er^{3+}.

ACKNOWLEDGMENTS

This work is supported by a Grant-in-Aid for Scientific Research from the Ministry of Education, Culture, Sports, Science and Technology, Japan.

*Author to whom correspondence should be addressed. Electronic address: fujii@eedept.kobe-u.ac.jp

[1] C. E. Chryssou, A. J. Kenyon, T. S. Iwayama, C. W. Pitt, and D. E. Hole, Appl. Phys. Lett. **75**, 2011 (1999).
[2] A. J. Kenyon, P. F. Trwoga, M. Federighi, and C. W. Pitt, J. Phys.: Condens. Matter **6**, L319 (1994).
[3] M. Fujii, M. Yoshida, Y. Kanzawa, S. Hayashi, and K. Yamamoto, Appl. Phys. Lett. **71**, 1198 (1997).
[4] M. Fujii, M. Yoshida, S. Hayashi, and K. Yamamoto, J. Appl. Phys. **84**, 4525 (1998).
[5] G. Franzò, V. Vinciguerra, and F. Priolo, Appl. Phys. A **69**, 3 (1999).
[6] P. G. Kik, M. L. Brongersma, and A. Polman, Appl. Phys. Lett. **76**, 2325 (2000).
[7] J. H. Shin, S.-Y. Seo, S. Kim, and S. G. Bishop, Appl. Phys. Lett. **76**, 1999 (2000).
[8] K. Watanabe, H. Tamaoka, M. Fujii, K. Moriwaki, and S. Hayashi, Physica E (Amsterdam) **13**, 1038 (2002).
[9] H. Han, S. Seo, and J. Shin, Appl. Phys. Lett. **79**, 4568 (2001).
[10] H. Han, S. Seo, J. Shin, and Namkyoo Park, Appl. Phys. Lett. **81**, 3720 (2002).
[11] D. Pacifici, G. Franzo, F. Priolo, F. Iacona, and L. DalNegro, Phys. Rev. B **67**, 245301 (2003).
[12] M. Fujii, K. Imakita, K. Watanabe, and S. Hayashi, J. Appl. Phys. **95**, 272 (2004).
[13] T. Förster, *Fluorenzenz Organische Verbindungen* (Vandenhoech and Ruprech, Gottingen, 1951).
[14] K. Imakita, M. Fujii, and S. Hayashi, Phys. Rev. B **71**, 193301 (2005).
[15] G. S. Agarwal and S. Dutta Gupta, Phys. Rev. A **57**, 667 (1998).
[16] T. Kobayashi, Q. Zheng, and T. Sekiguchi, Phys. Rev. A **52**, 2835 (1995).
[17] G. Kurizki, A. G. Kofman, and V. Yudson, Phys. Rev. A **53**, R35 (1996).
[18] G. Kurizki and A. Z. Genack, Phys. Rev. Lett. **61**, 2269 (1988).
[19] M. Hopmeier, W. Guss, M. Deussen, E. O. Gobel, and R. F. Mahrt, Phys. Rev. Lett. **82**, 4118 (1999).
[20] P. Andrew and W. L. Barnes, Science **290**, 27 (2000).
[21] M. J. A. de Dood, J. Knoester, A. Tip, and A. Polman, Phys. Rev. B **71**, 115102 (2005).
[22] G. Mauckner, K. Thonke, T. Baier, T. Walter, and R. Sauer, J. Appl. Phys. **75**, 4167 (1994).
[23] R. R. Chance, A. Prock, and R. Silbey, Adv. Chem. Phys. **37**, 1 (1978).
[24] J. Kalkman, Ph.D. thesis, Utrecht University, 2005.
[25] W. L. Barnes, J. Mod. Opt. **45**, 661 (1998).
[26] David W. Lynch and W. R. Hunter, in *Handbook of Optical Constants in Solid*, edited by Edward D. Palik (Academic, New York, 1985).
[27] P. A. Snow, E. K. Squire, P. St. J. Russell, and L. T. Canham, J. Appl. Phys. **86**, 1781 (1999).
[28] J. Kalkman, L. Kuipers, and A. Polman, Appl. Phys. Lett. **86**, 41113 (2005).
[29] P. T. Worthing, R. M. Amos, and W. L. Barnes, Phys. Rev. A **59**, 865 (1999).
[30] P. Andrew and W. L. Barnes, Phys. Rev. B **64**, 125405 (2001).